Surface Induced Dissociation in Tandem Mass spectrometry

Ananya Baksi
15-11-14

Tandem Mass spectrometry (MSn)

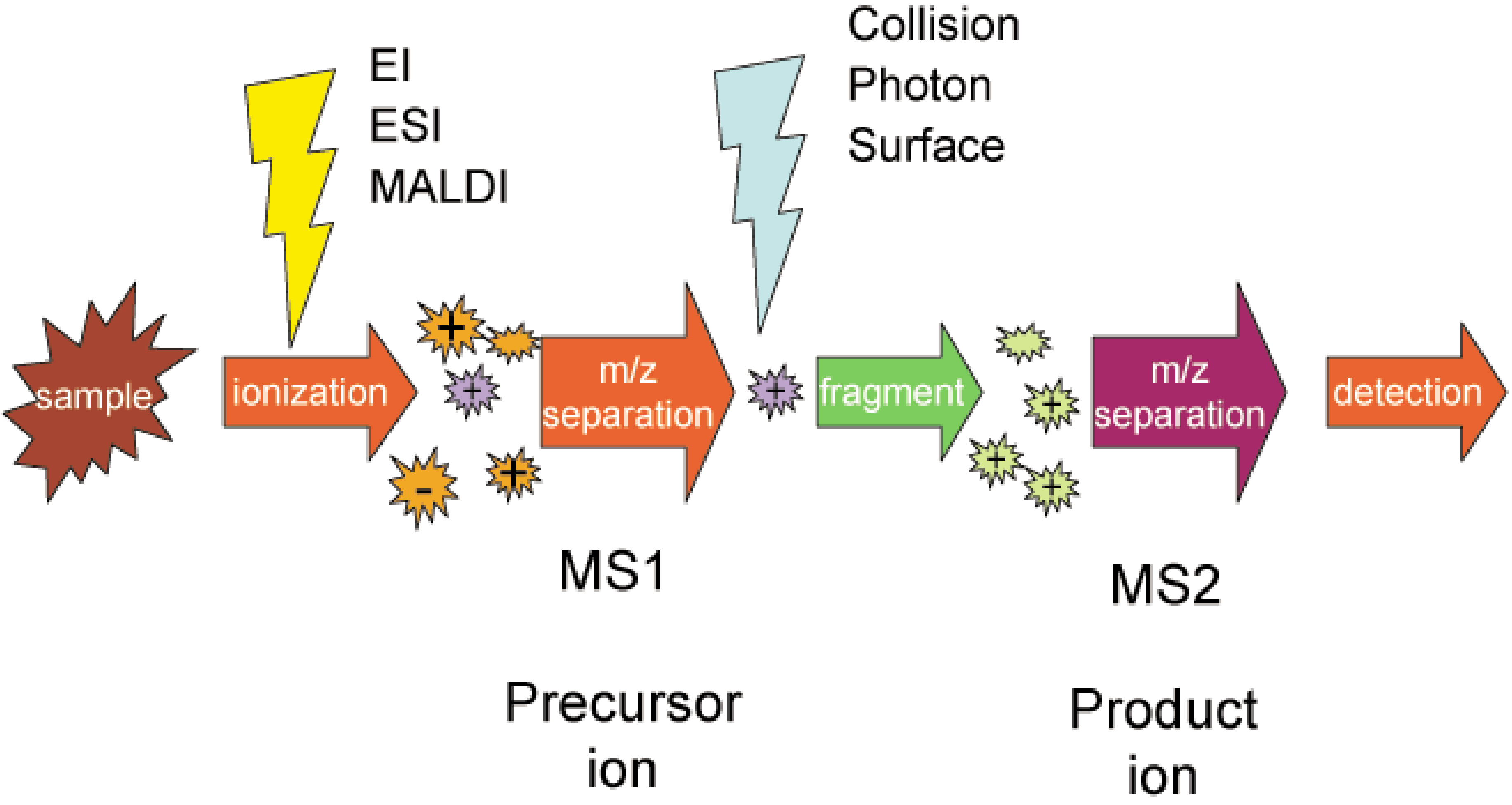

sample

ionization

EI
ESI
MALDI

m/z separation

MS1

Precursor ion

Collision
Photon
Surface

fragment

m/z separation

MS2

Product ion

detection

Different Modes of Fragmentation

1. In-source fragmentation

2. Collision-induced dissociation (CID)

$$AB++M \longrightarrow A+B++M$$

3. Electron capture and transfer methods

3.1 *Electron capture dissociation (ECD)*

$$[AB+nH]n+ +e- \longrightarrow [AB+(n-1)H](n-1)+]* \longrightarrow \text{Fragments}$$

3.2 Electron transfer dissociation (ETD)

$$[AB+nH]n+ +A- \longrightarrow [AB+(n-1)H](n-1)+]* +A \longrightarrow \text{Fragments}$$

3.3 Negative electron transfer dissociation

$$[AB-nH]n- +A+ \longrightarrow [AB+(n-1)H](n+1)-]* +A \longrightarrow \text{Fragments}$$

3.4 Electron-detachment dissociation (EDD)

4. Photodissociation

4.1 Infrared multiphoton dissociation

$$AB++h\upsilon \longrightarrow A+B+$$

4.2 Blackbody infrared radiative dissociation

5. Surface induced dissociation (SID)

Different Modes of Fragmentation

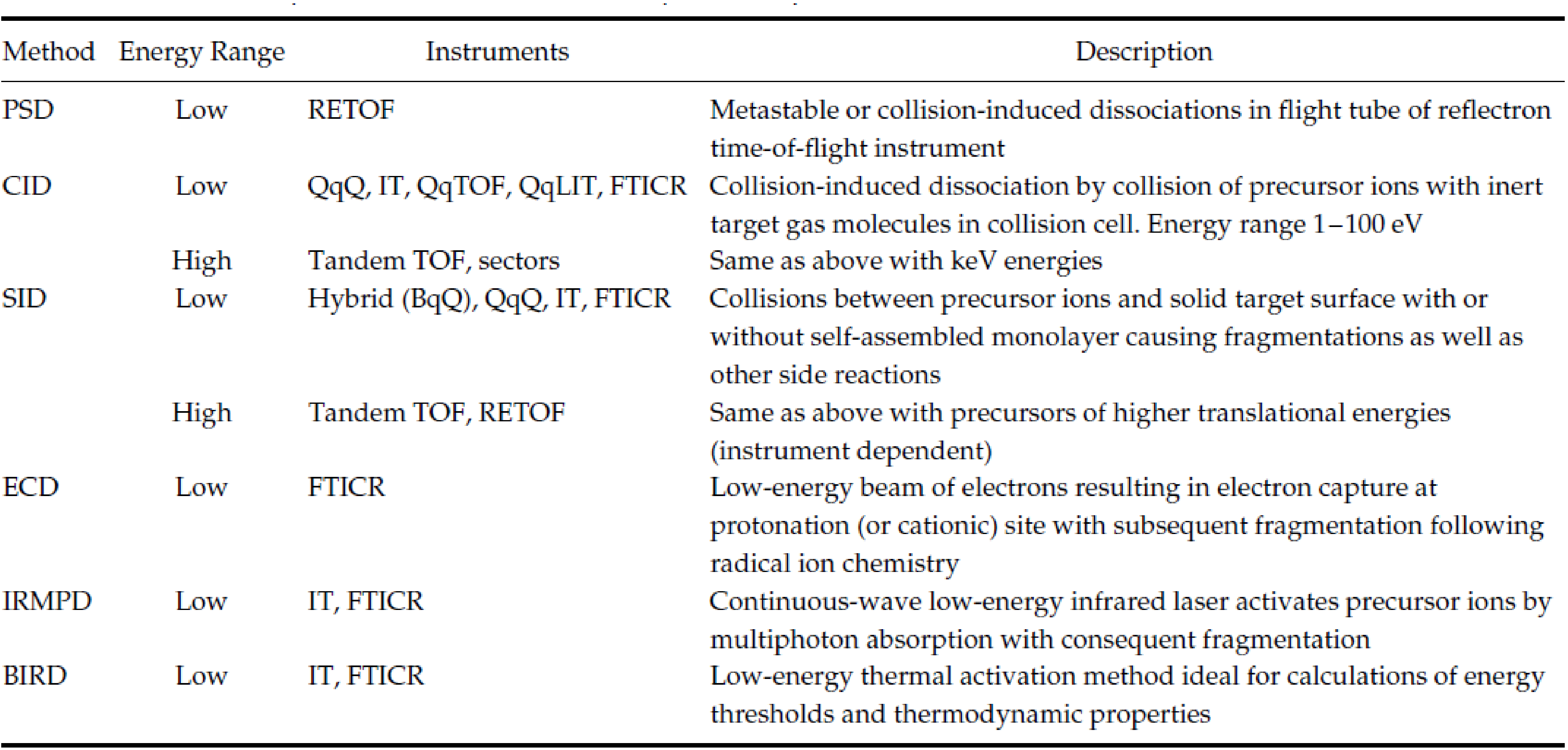

Method	Energy Range	Instruments	Description
PSD	Low	RETOF	Metastable or collision-induced dissociations in flight tube of reflectron time-of-flight instrument
CID	Low	QqQ, IT, QqTOF, QqLIT, FTICR	Collision-induced dissociation by collision of precursor ions with inert target gas molecules in collision cell. Energy range 1–100 eV
	High	Tandem TOF, sectors	Same as above with keV energies
SID	Low	Hybrid (BqQ), QqQ, IT, FTICR	Collisions between precursor ions and solid target surface with or without self-assembled monolayer causing fragmentations as well as other side reactions
	High	Tandem TOF, RETOF	Same as above with precursors of higher translational energies (instrument dependent)
ECD	Low	FTICR	Low-energy beam of electrons resulting in electron capture at protonation (or cationic) site with subsequent fragmentation following radical ion chemistry
IRMPD	Low	IT, FTICR	Continuous-wave low-energy infrared laser activates precursor ions by multiphoton absorption with consequent fragmentation
BIRD	Low	IT, FTICR	Low-energy thermal activation method ideal for calculations of energy thresholds and thermodynamic properties

Dietrich A. Volmer *et al., J. Mass Spectrom. 2004; 39, 1091–1112*

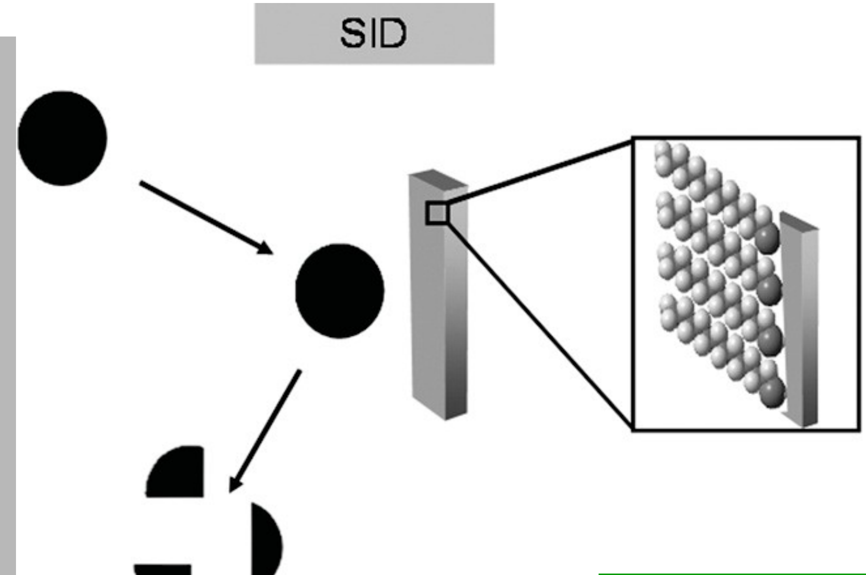

Diagram of surface-induced dissociation where surface collision event deposits energy into the precursor ion. Collisions can generate fragment ions, neutralized precursor molecules, sputtered surface atoms, and ion–surface reaction products. Inset shows an all-trans configuration alkanethiolate (e.g., CH3(CH2)11SAu) self-assembled monolayer on gold.

J Am Soc Mass Spectrom 2008, 19, 190–208

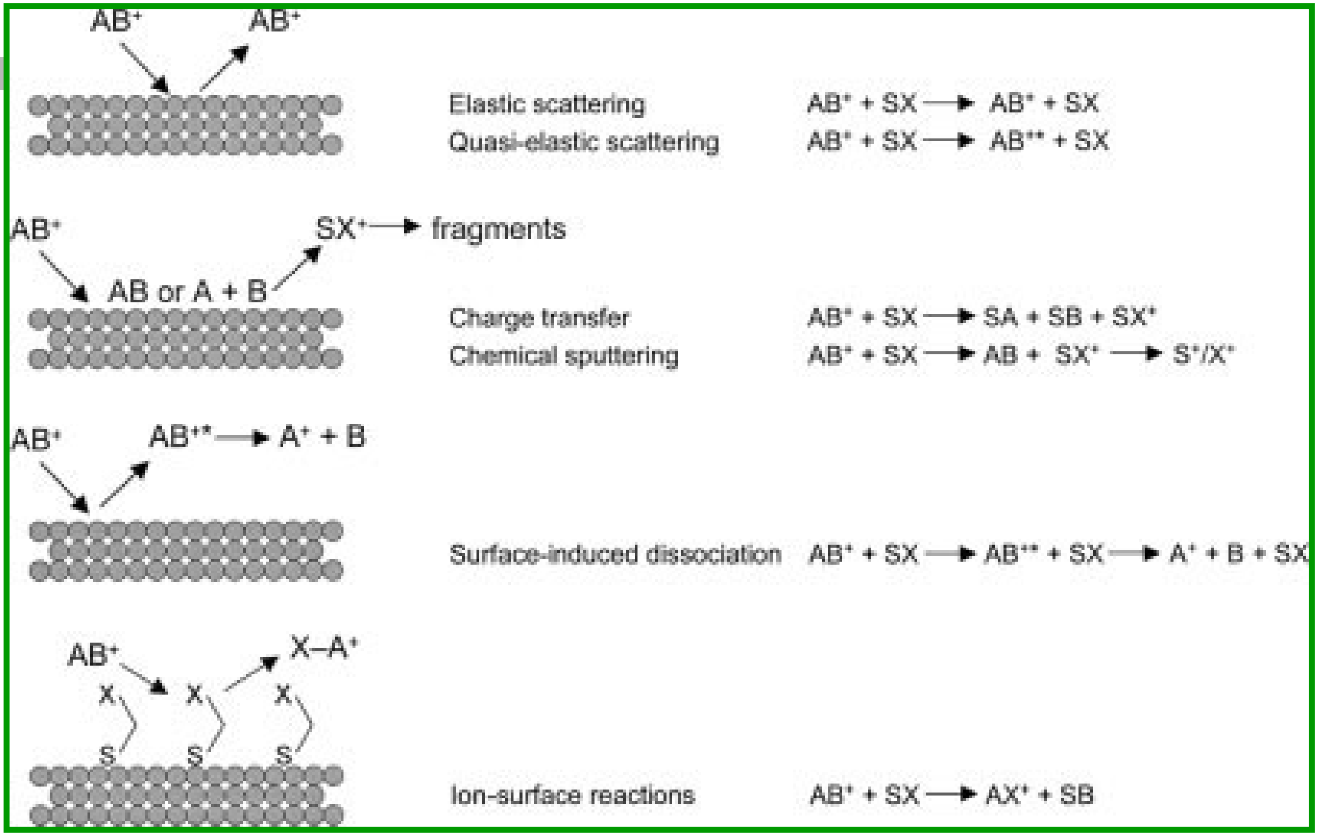

Elastic scattering $AB^+ + SX \longrightarrow AB^+ + SX$

Quasi-elastic scattering $AB^+ + SX \longrightarrow AB^{+*} + SX$

Charge transfer $AB^+ + SX \longrightarrow SA + SB + SX^+$

Chemical sputtering $AB^+ + SX \longrightarrow AB + SX^+ \longrightarrow S^+/X^+$

Surface-induced dissociation $AB^+ + SX \longrightarrow AB^{+*} + SX \longrightarrow A^+ + B + SX$

Ion-surface reactions $AB^+ + SX \longrightarrow AX^+ + SB$

CID Vs. SID

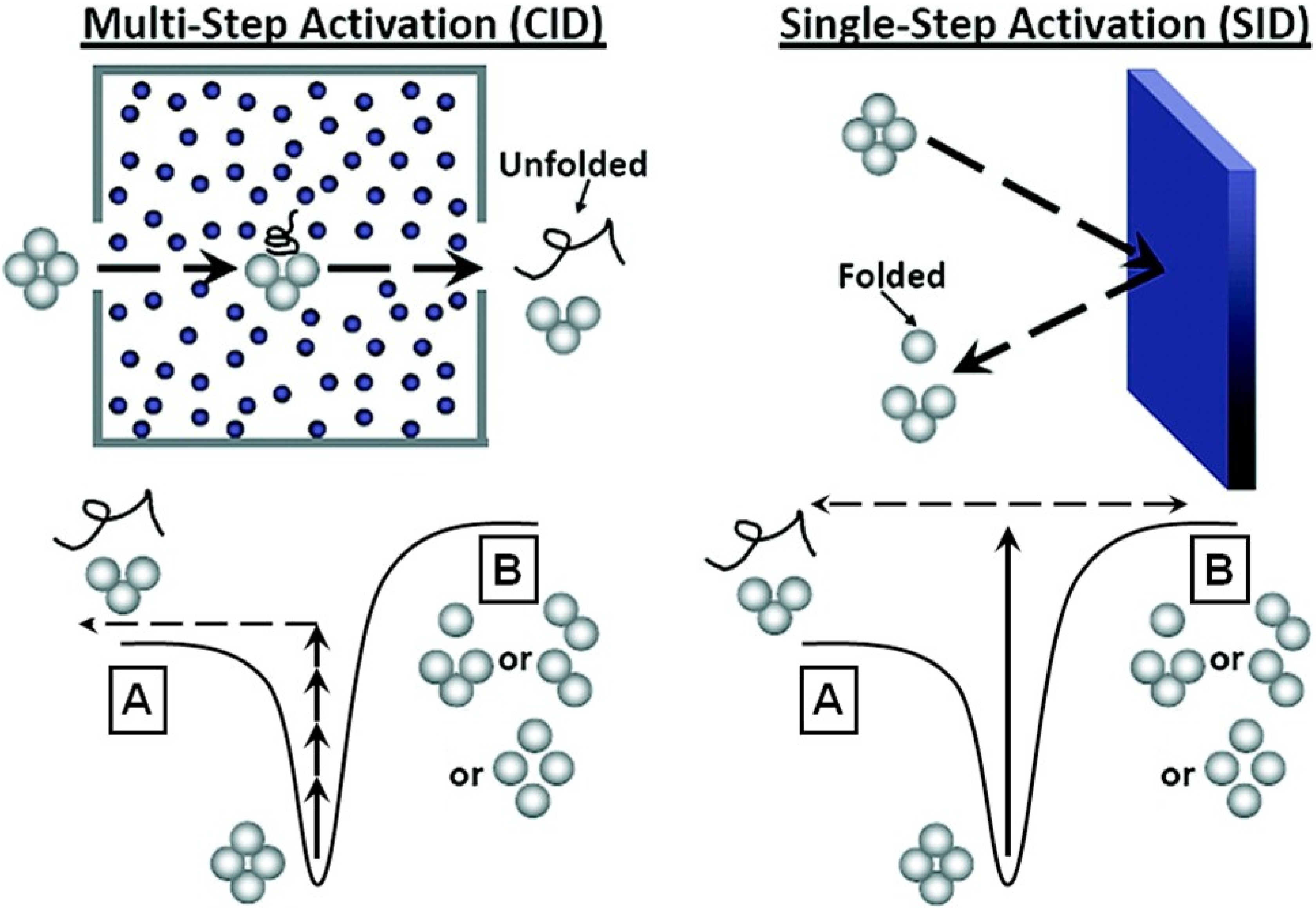

Acc. Chem. Res., dx.doi.org/10.1021/ar400223t

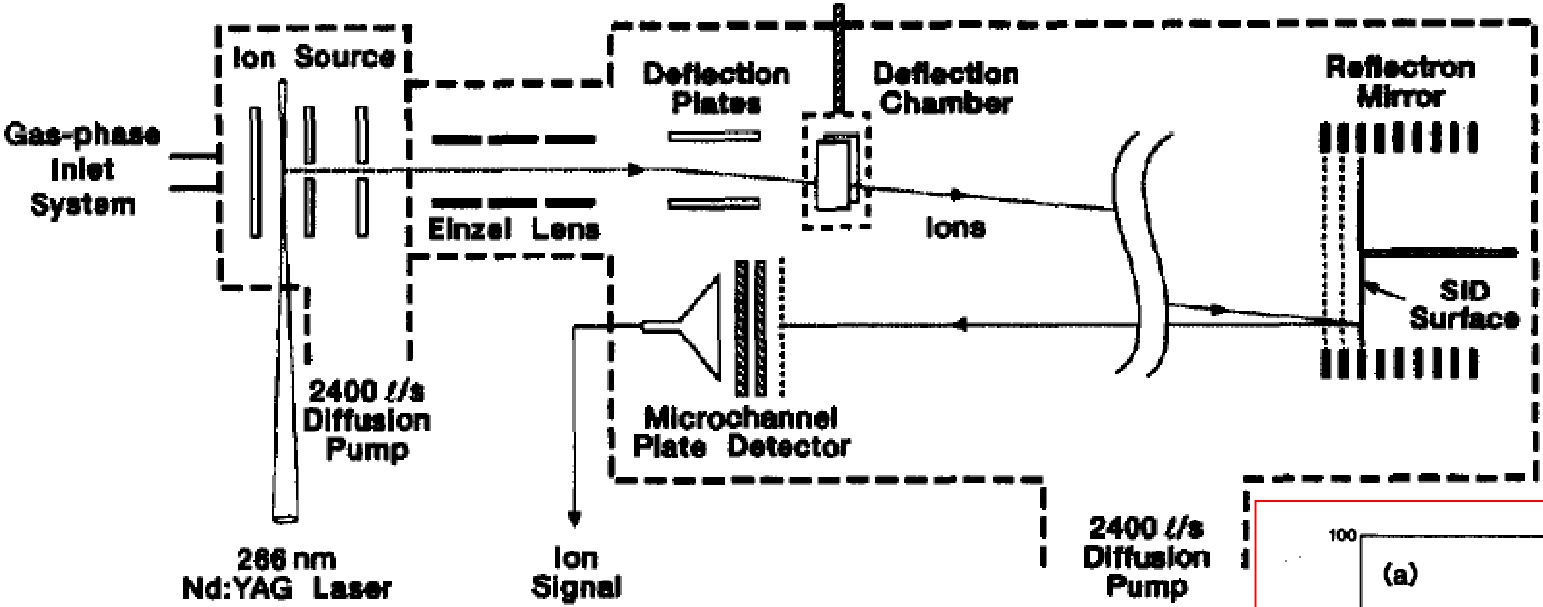

Fig. 1. Schematic of the tandem TOF mass spectrometer for SID.

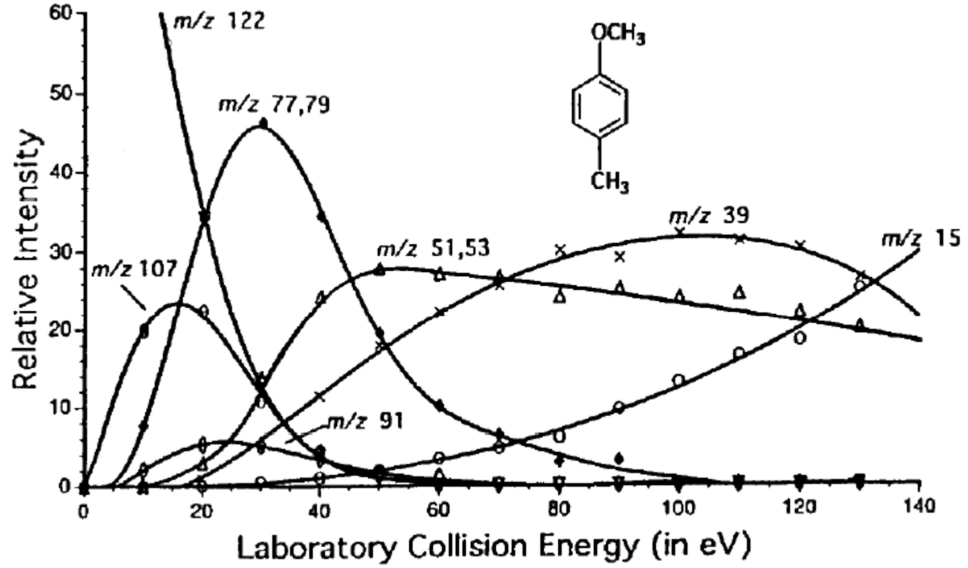

Fig. 6. SID breakdown curve for the 4-methylanisole molecular ion, $C_8H_{10}O^{\cdot +}$.

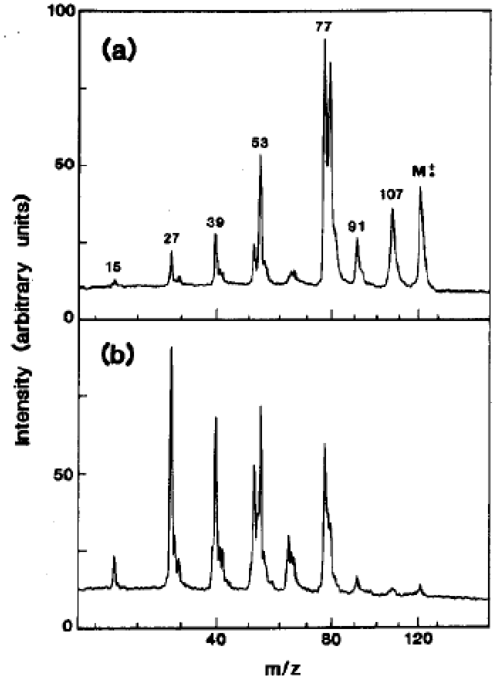

Fig. 5. SID spectra of the molecular ion of 4-methylanisole, $C_8H_{10}O^{\cdot +}$, at 30 (a) and 50 eV (b) collision energies.

Richard N. Zare *et al., Inl. J. Mass Spectrom. Ion Processes, 1993, 123, 231-241*

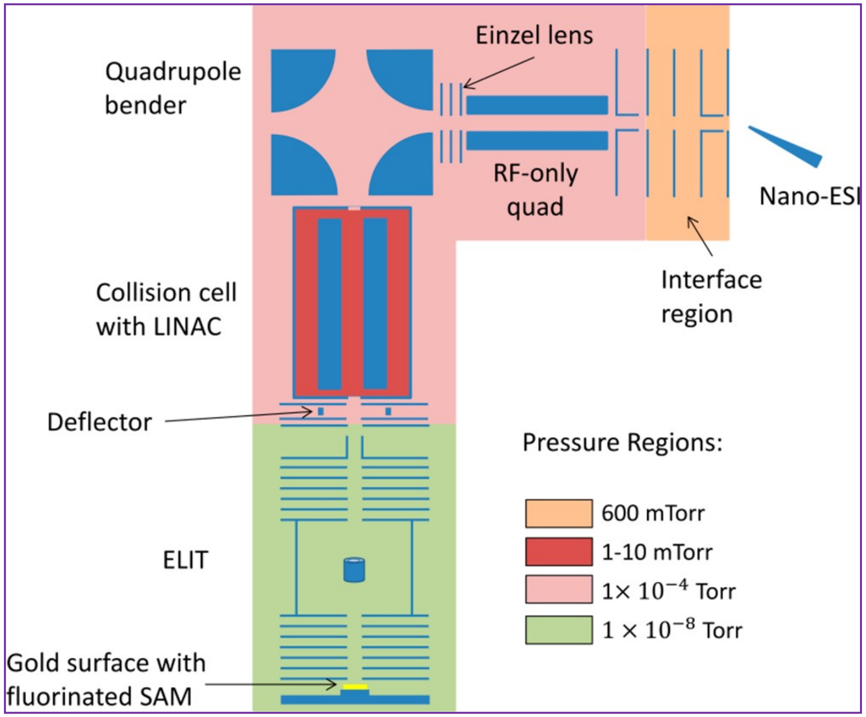

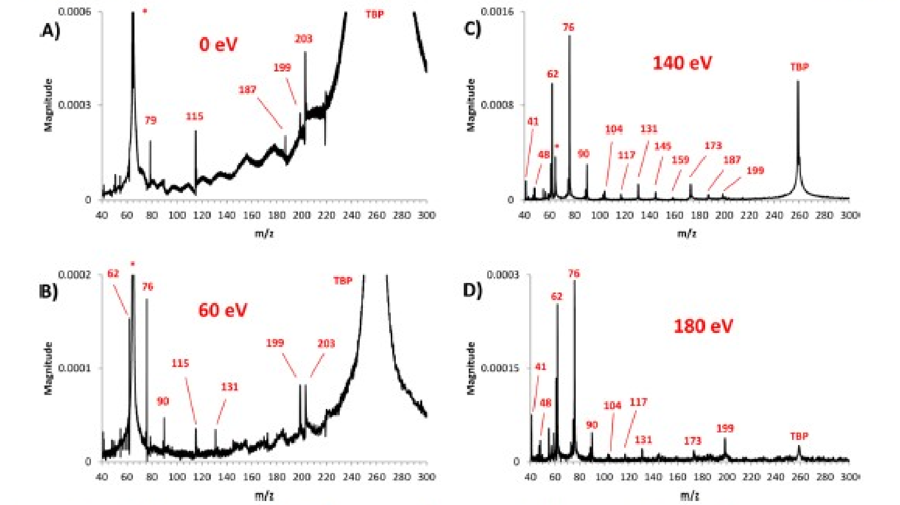

Figure 6. Spectra obtained after performing SID of TBP at various collision energies. In (A), ions are simply reflected leading to an intense precursor ion signal and much weaker signals from contaminants. At 60 eV, fragment ions begin to appear as shown in (B). 140 eV provides the highest signals for fragment ions as shown in (C). Increasing the collision energy to 180 eV simply results in decreased intensities for all ions as shown in (D).

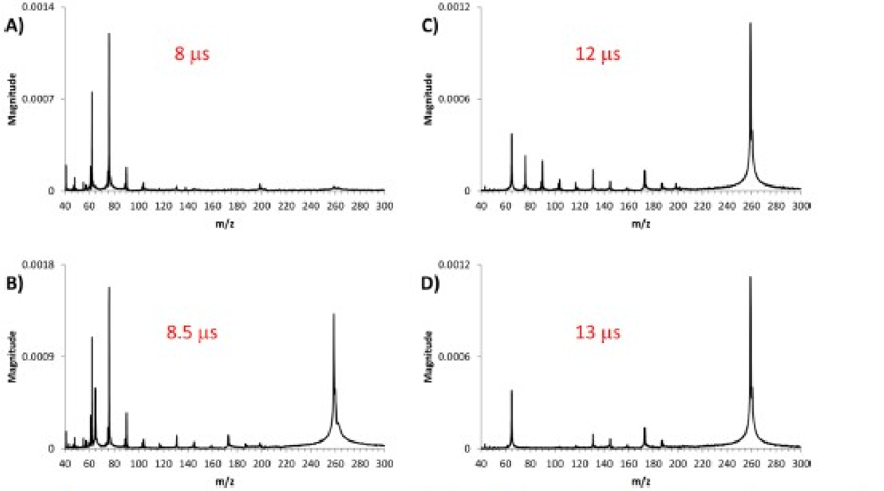

Figure 7. TBP product ion spectra recorded while varying the width of the pulse that makes the surface available for collision (see Figure 6C for peak labels). Similar product ion spectra are produced for pulse widths between 8.5 and 12 μs. Discrimination against high *m*/*z* and low *m*/*z* products is apparent at lower and higher pulse widths, respectively (see text for details).

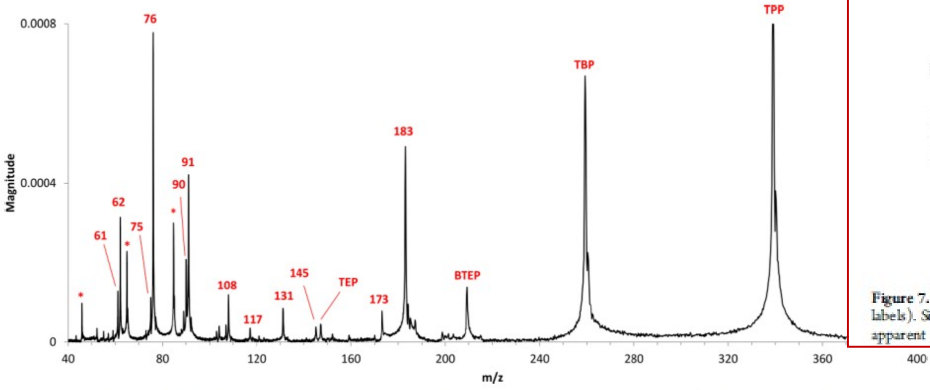

Figure 4. Spectrum obtained after SID (collision energy of 140 eV) of the mixture of TEP, BTEP, TBP, and TPP. Inelastically scattered precursor ions are identified while fragments are labeled with their nominal *m*/*z*. Harmonics of intense peaks are labeled with asterisks.

Scott A. McLuckey *et al*., *Anal. Chem.* 2014, 86, 8822−8828

Some Examples

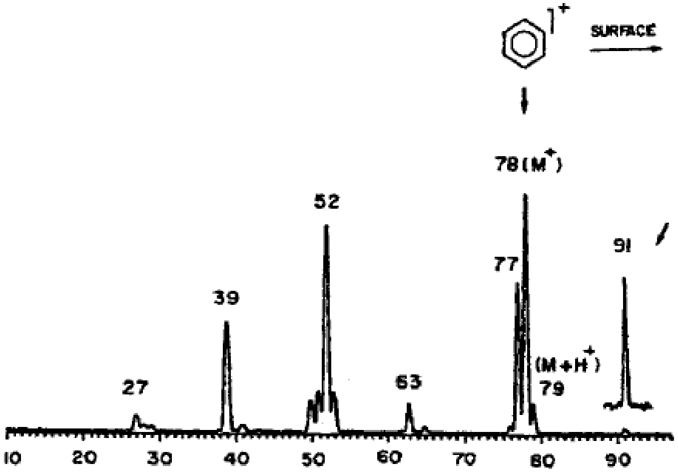

Figure 11. An SID spectrum is shown for the benzene molecular ion. Ion–surface reactions are apparent by the presence at *m/z* 91, corresponding to the stable tropylium ion. This product is formed by initial methyl abstraction from the adsorbate present on the surface target, followed by the loss of a hydrogen molecule (H_2). Note also that *m/z* 78 corresponds to the protonated ion, formed by hydrogen abstraction from the surface, another common ion–surface reaction seen in SID.

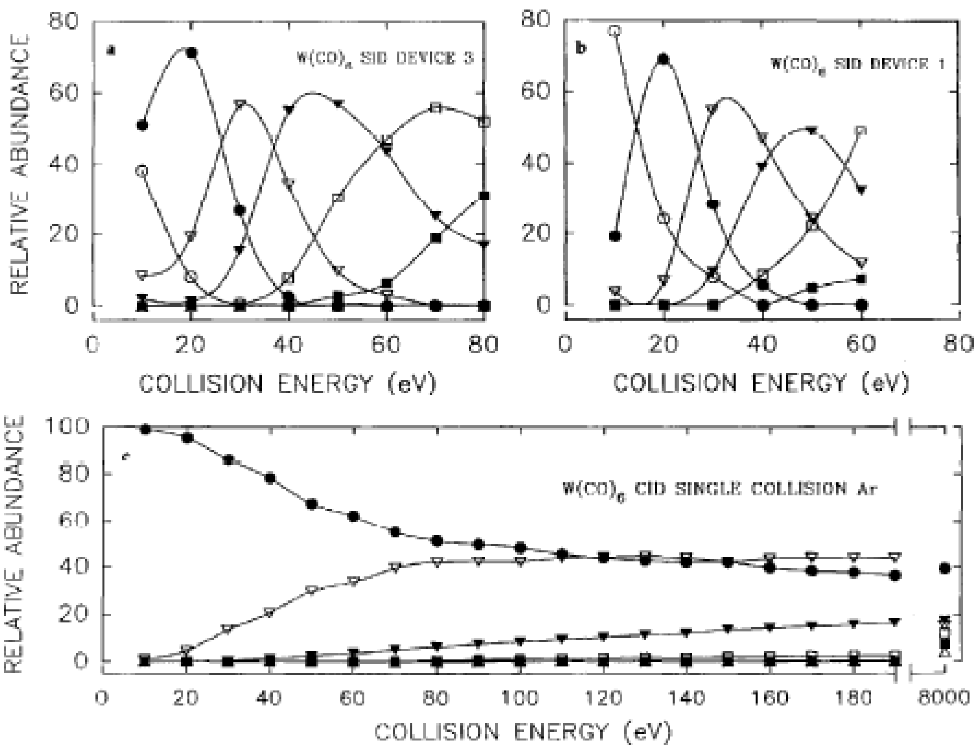

Figure 3. Energy-resolved tandem mass spectra of $W(CO)_6$ obtained by using (a) SID device 3, (b) SID device 1, (c) CID with Ar at 10–200 eV (single-collision conditions) and CID with He at 8000 eV. (○) $W(CO)_6^{+\bullet}$; (●) $W(CO)_5^{+\bullet}$; (▽) $W(CO)_4^{+\bullet}$; (▼) $W(CO)_3^{+\bullet}$; (□) $W(CO)_2^{+\bullet}$; (■) $W(CO)^{+\bullet}$.

Some Examples

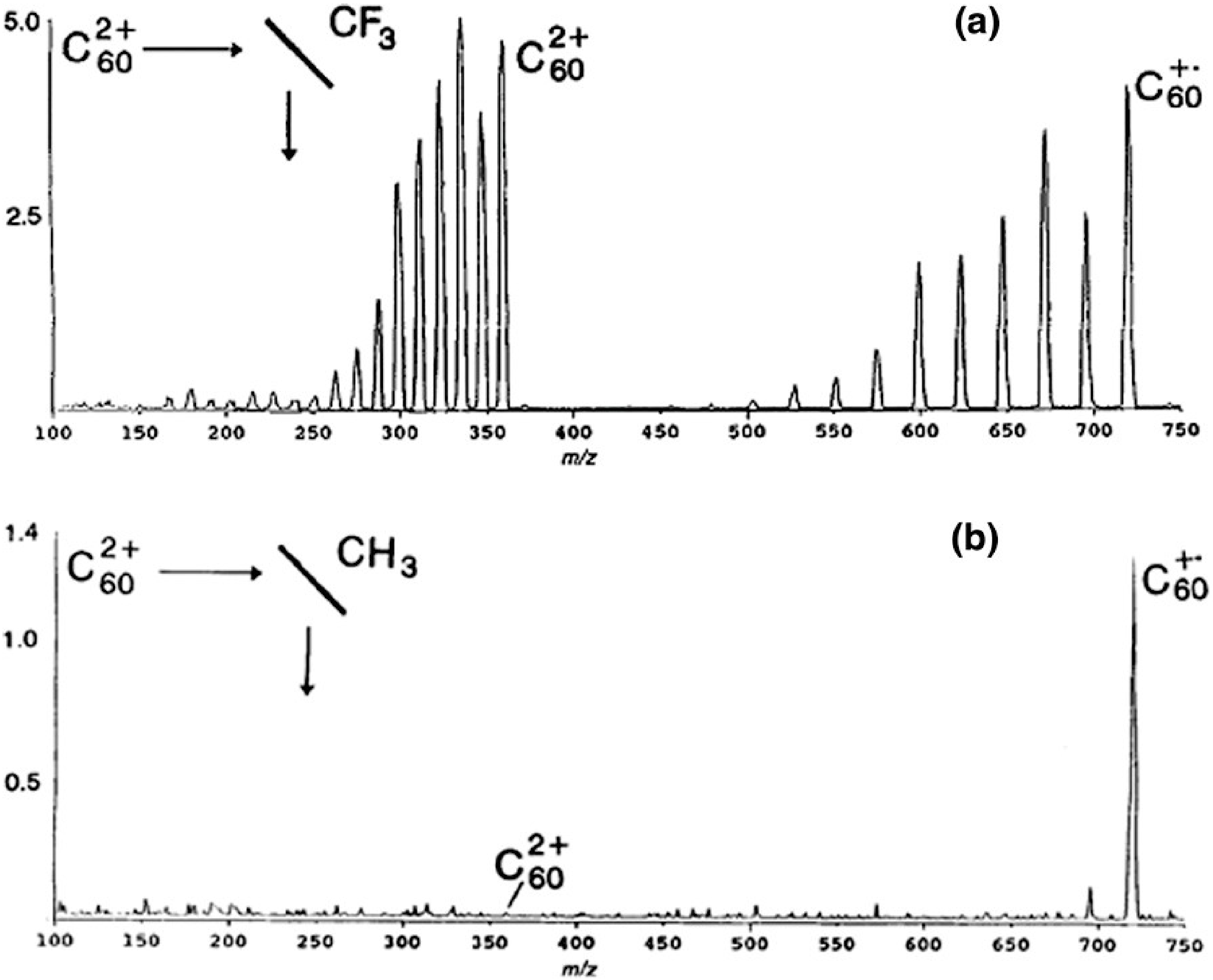

SID of C60 at 250eV collision energy on (a) fluorocarbon and (b) hydrocarbon self-assembled monolayers (SAMs). Collisions on the hydrocarbon surface show significant amounts of one electron charge reduction whereas collisions on the fluorinated surface show fragmentation of both the charge reduced ion and the doubly charged precursor.

Rapid Commun. Mass Spectrom. 1993, 7, 693–699.

Some Examples

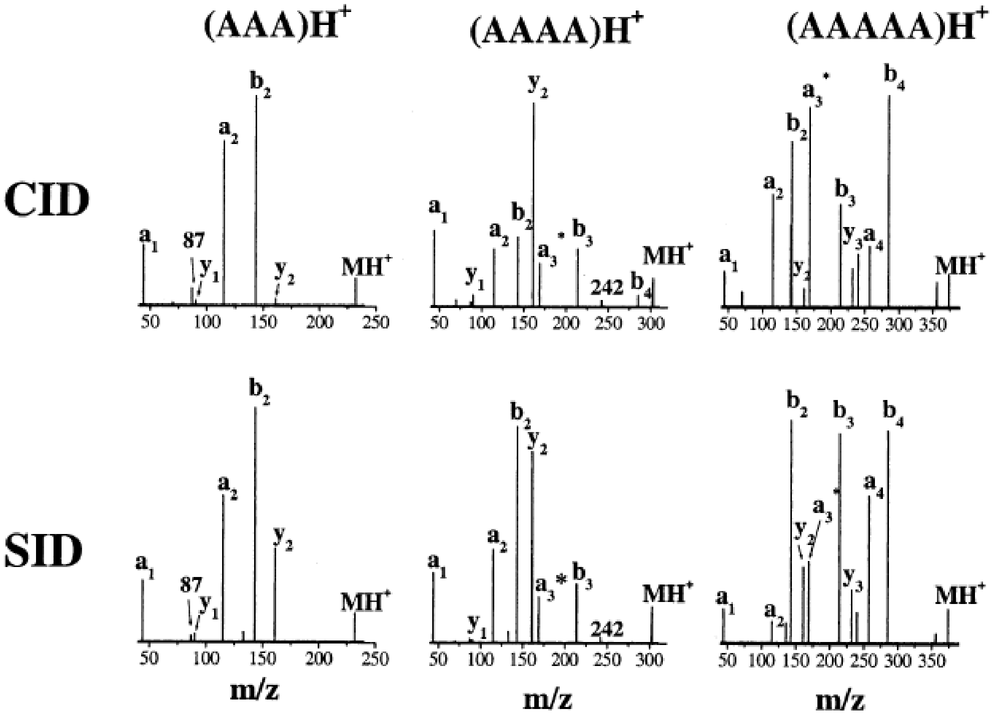

MS/MS spectra of small protonated polyalanines obtained using SORI-CID (top panel) and the matching FT-ICR SID spectra (bottom panel).

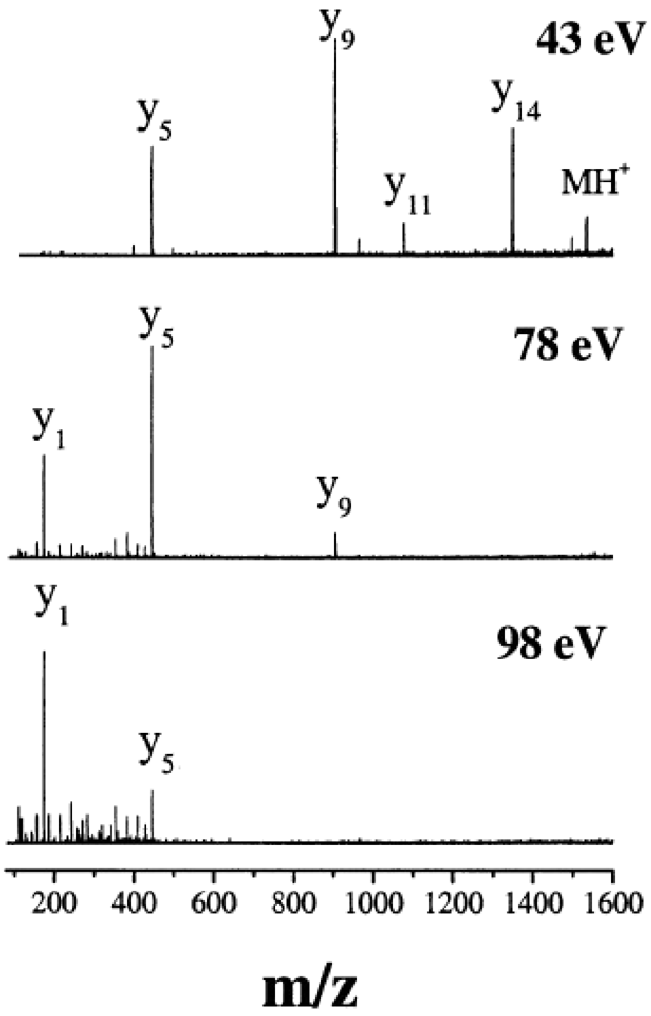

FT-ICR SID spectra of singly protonated Fibrinopeptide at several collision energies and reaction delay of 1 s.

J Am Soc Mass Spectrom 2003, 14, 1340–1347

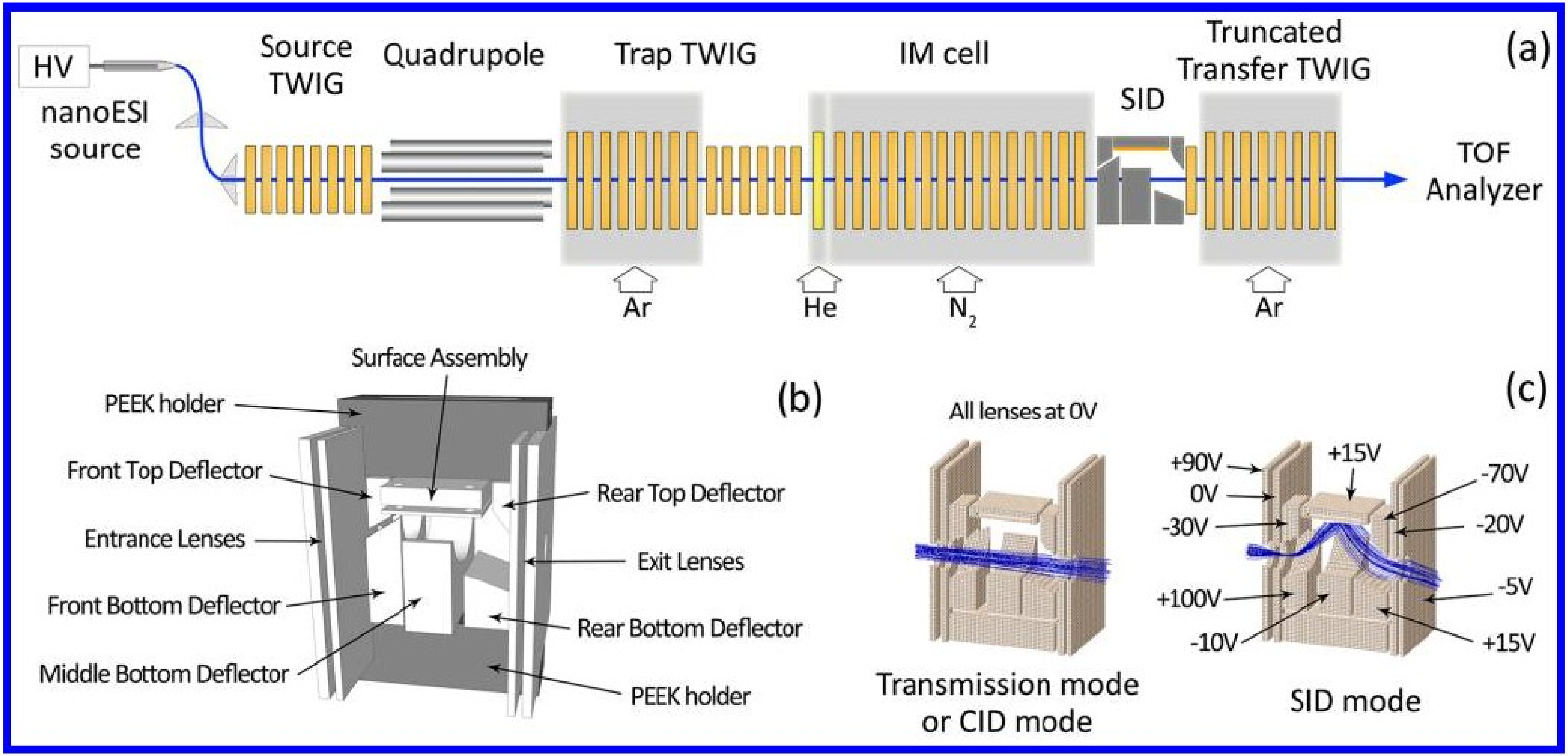

Anal. Chem. 2012, 84, 6016−6023

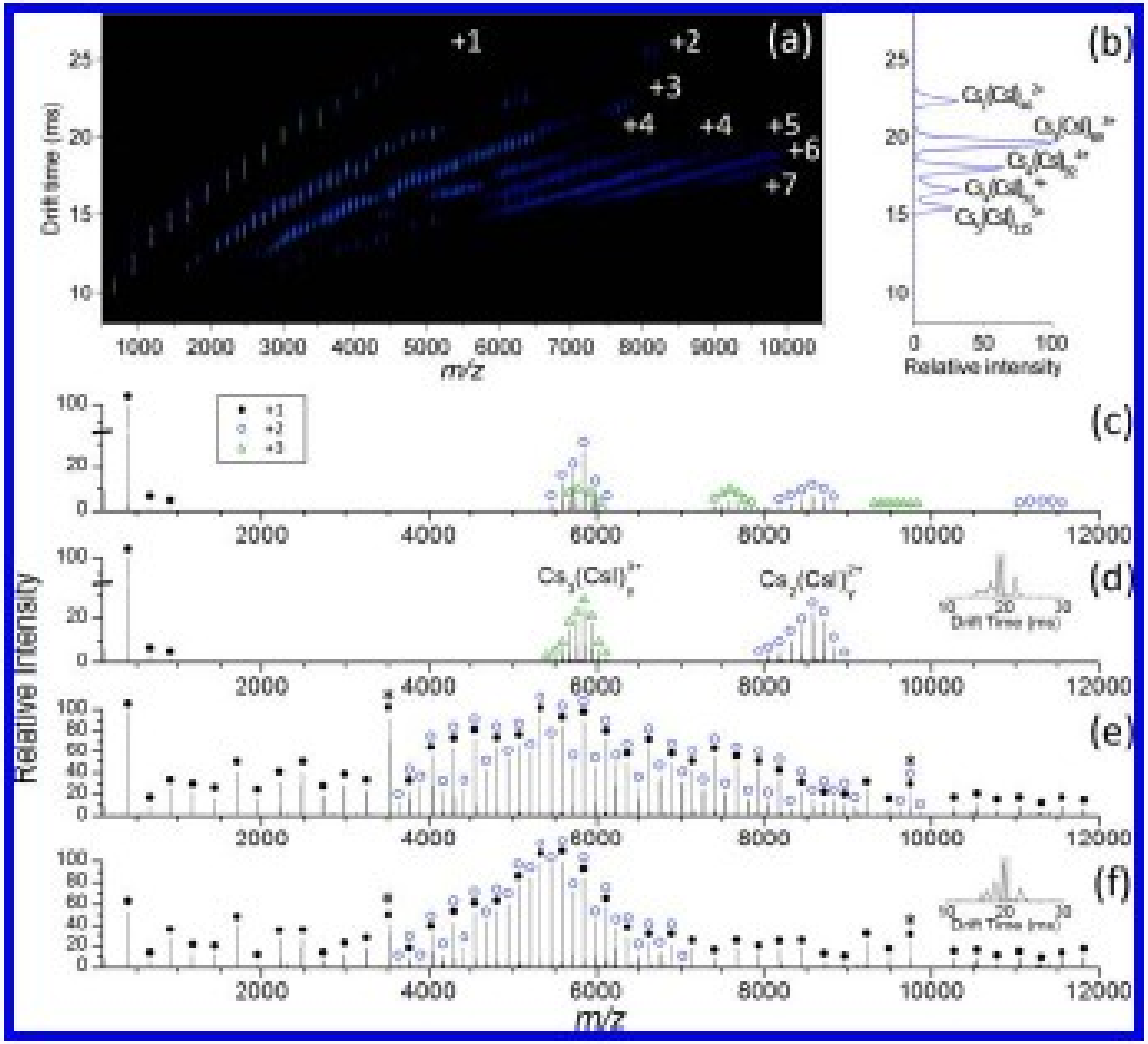

Figure 2. (a) IM-MS spectrum of CsI clusters. The brightness of the spots in the spectrum indicates the intensity of the species. (b) Drift time distribution of *m/z* 6108, which consists of overlapping multiply charged ions. (c) Convoluted CID spectrum at 65 V of all the ions $Cs_a(CsI)_{23a}{}^{a+}$ overlapping at *m/z* 6108.5. (d) Extracted CID spectrum of $Cs_3(CsI)_{69}{}^{3+}$ at 65 V. The inset shows the drift time distribution of CID products, and the shaded peak is the one whose spectrum is extracted here. (e) Convoluted SID spectrum at 65 V of all the ions $Cs_a(CsI)_{23a}{}^{a+}$ overlapping at *m/z* 6108.5. (f) Extracted SID spectrum at 65 V of $Cs_3(CsI)_{69}{}^{3+}$. The inset is the drift time distribution of all SID products from the multiply charged species, and the shaded peak corresponds to $Cs_3(CsI)_{69}{}^{3+}$. The asterisk-labeled peaks correspond to magic number clusters.

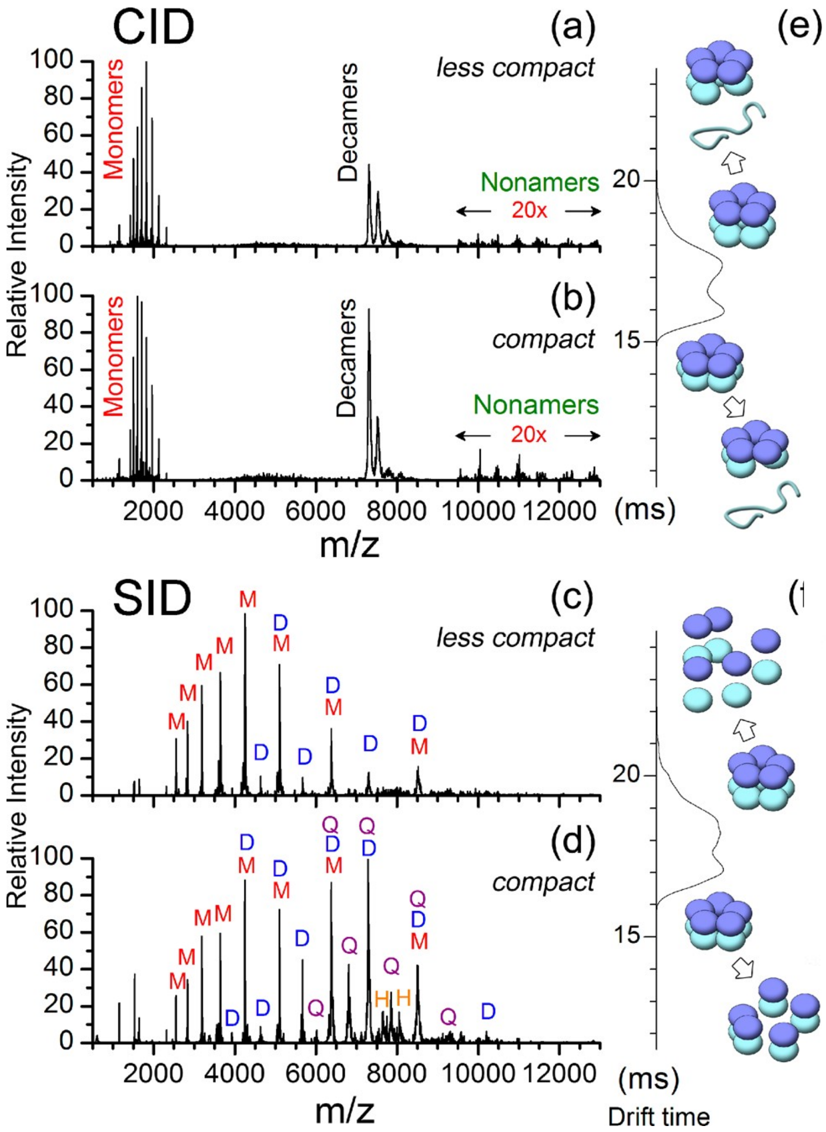
CID
(a)
less compact
(b)
compact
(e)
Relative Intensity
Monomers
Decamers
Nonamers
20x
m/z
(ms)
SID
(c)
less compact
(d)
compact
(f
M
D
Q
H
Drift time
2000
4000
6000
8000
10000
12000
0
20
40
60
80
100
15
20

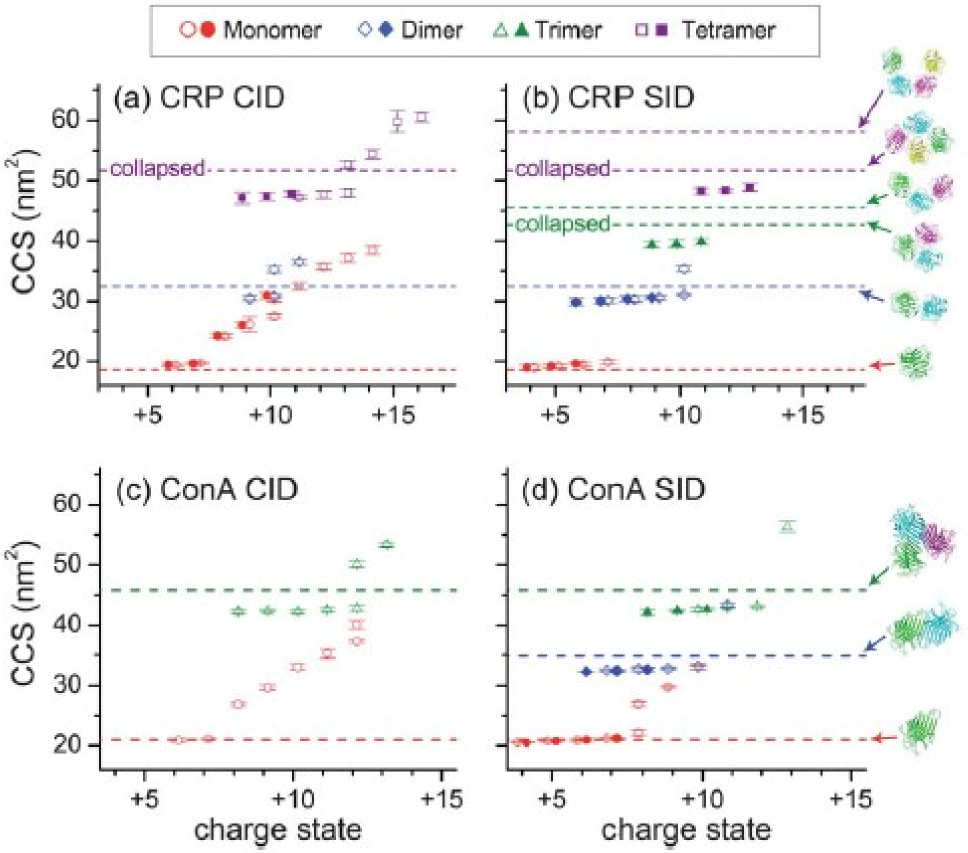
○● Monomer
◇◆ Dimer
△▲ Trimer
□■ Tetramer
(a) CRP CID
(b) CRP SID
(c) ConA CID
(d) ConA SID
collapsed
CCS (nm^2)
charge state
+5
+10
+15
20
30
40
50
60

Advantages of SID over CID

- ✓Single step activation
- ✓Energy efficient
- ✓Dissociation of substrate is dependent on the surface. By simply changing the surface mode of dissociation can be changed
- ✓Efficient to understand structural information of large molecules.

Thank You!